

Rotations of brittle particles during plastic deformation of ductile alloys

H. Agrawal^a, A.M. Gokhale^{a,*}, S. Graham^b, M.F. Horstemeyer^b, D.J. Bamman^b

^a School of Materials Science and Engineering, Georgia Institute of Technology, Atlanta, GA 30332-0245, USA

^b Sandia National Laboratories, PO Box 969, Livermore, CA 94551-10969, USA

Received 8 May 2001; received in revised form 30 July 2001

Abstract

Experimental evidence is presented to show that significant rotations of brittle phase inclusions of a Fe-rich intermetallic phase occur during plastic deformation on an Al–Mg–Si base wrought aluminum alloy. The particle rotations are quantitatively characterized, for uniaxial tension, compression, torsion, and notch-tension test specimens strained to different strain levels. The particle rotations are monitored by measuring the morphological orientation distribution function of the particles. Significant particle rotations occur under all loading conditions. The morphological orientation distribution function evolves with plastic strain under uniaxial tension, compression, and torsion. The particles tend to align themselves in the direction parallel to applied (or induced) tensile stress for deformation under tension and compression. In the case, of torsion test specimens, at least up to 98% torsion strain, the particles tend to align along the direction at an angle of 45° to torsion axis. © 2002 Elsevier Science B.V. All rights reserved.

Keywords: Aluminum alloys; Damage; Microstructure; Alignment; Particle rotations

1. Introduction

Many structural alloys contain inclusions/particles of brittle phases dispersed in a ductile matrix. In such microstructures, particle cracking is an important damage initiation mode [1–7]. Micro-voids grow around the cracked brittle phase particles. The subsequent void growth and coalescence lead to the final failure of the material. Numerous theories of particle fracture-based damage initiation have been reported in the literature [8–17]. Particle cracking has also been studied experimentally in several alloy systems [1–7]. Experimental observations as well as theoretical predictions indicate that particle cracking is a strong function of particle orientations with respect to the loading direction, particularly when the particles have non-equiaxed shapes [3,4,8,9].

The particle cracking based damage evolution theories [8–17] implicitly assume that the brittle particles remain stationary when the solid matrix is plastically deformed

under an applied load, and therefore, the particle orientations do not change with the plastic strain. The particle rotations can bring the particles in the orientation ranges that facilitate particle cracking. Therefore, particle rotations should be accounted for in the damage evolution models, if significant particle rotations do occur.

It is the purpose of this contribution to present quantitative experimental data, which clearly reveal that, depending on the stress state, strain path, and microstructural anisotropy, significant brittle particle rotations occur that lead to measurable changes in the morphological orientation distribution function of the particles. The morphological orientation distribution of the brittle particles evolves with strain, which is in turn expected to affect the strain/stress dependence of the fraction of cracked particles, and consequently, the damage evolution.

Theoretical analysis of brittle particle rotations in solid polycrystalline matrices has not been reported in the literature. However, particle rotations in viscous fluid matrices have been modeled. Jeffery [18] has developed equations for the motion of a suspended rigid ellipsoid in a Newtonian fluid. Prager [19] has given

* Corresponding author. Tel.: +1-404-894-2887; fax: +1-404-894-9140.

E-mail address: arun.gokhale@mse.gatech.edu (A.M. Gokhale).

Table 1
Chemical composition of 6061 Al-alloy

Element	Zn	Ti	Si	Mn	Mg	Fe	Cu	Cr	Al
Wt pct	0.02	0.01	0.65	0.04	1.06	0.37	0.28	0.2	Bal.

equations determining the preferred direction adopted by a suspension of non-interacting particles in the shape of dumbbells. Erickson [20] has utilized director theory to develop a theory describing the motion of liquid crystals, and Hand [21] developed a theory describing anisotropic fluids that described the reorientation of ellipsoidal particles in a dilute suspension. More recently, Advani and Tucker [22] have used sets of even ordered tensors to describe the probability distribution function of fiber reorientation in suspensions and composites containing short fibers. Prantil [23] used an approach analogous to Advani and Tucker to describe the reorientation of grains in the finite deformation of polycrystalline materials undergoing double planar slip. Therefore, brittle particle rotations during deformation of polycrystalline alloys are expected on the basis of plasticity and flow considerations.

Experimental observations on rotations/alignment of whiskers during deformation of non-crystalline polymer matrix composites have been reported. Further, rotations/alignments of short fibers/whiskers during uniaxial superplastic elongation of ductile matrices, induced by cyclic phase changes due to thermal cycling, have been observed [24,25]. Recently, Schuh and Dunand [25] have characterized rotations of TiB needles during superplastic deformation of a Ti-alloy matrix composite induced by thermal cycling around the alloy's phase transformation temperature range. However, there are no earlier quantitative experimental data on rotations of brittle particles/inclusions during deformation of polycrystalline alloys involving different loading conditions and stress states. Further, the link between such particle rotations (if significant rotations occur) and stress/strain dependent damage nucleation due to cracking has not been recognized.

In the present work, the experiments have been performed on a commercial 6061 Al-alloy, which is a typical wrought aluminum alloy. The morphological orientation distribution of Fe-based brittle intermetallic particles in the 6061 alloy is quantitatively characterized as function of strain under tension, compression, torsion, and notch-tension loading conditions. It is demonstrated that the morphological orientation distribution of the Fe-base intermetallic particles changes significantly at large plastic strains; the extent and nature of the changes orientation distribution function strongly depend on the strain, loading condition, and stress-state.

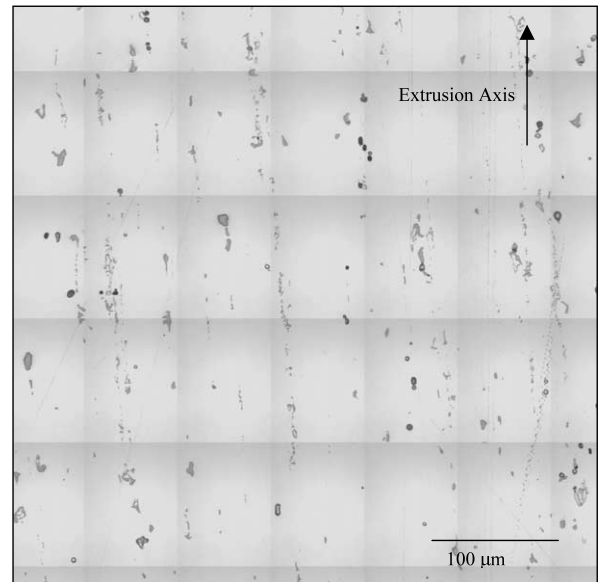


Fig. 1. Digitally compressed montage of $500 \times 500 \mu\text{m}^2$ area in an unstrained 6061 Al-alloy, originally grabbed at $50 \times$ objective magnification.

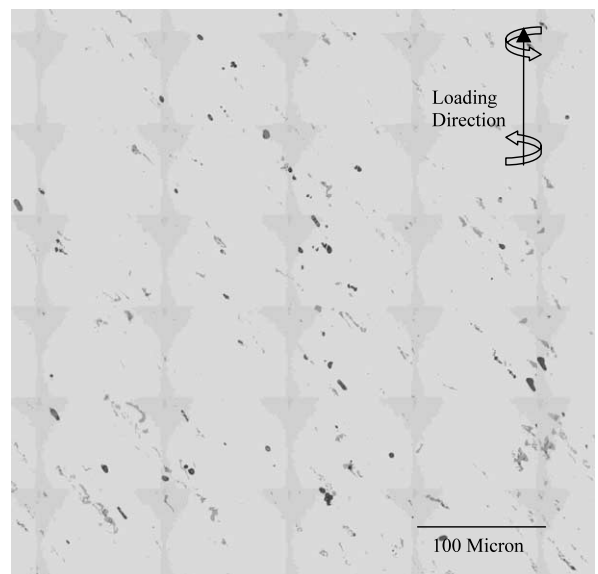


Fig. 2. Digitally compressed montage of $500 \times 500 \mu\text{m}^2$ area in 98% torsion 6061 Al-alloy specimen, originally grabbed at $50 \times$ objective magnification.

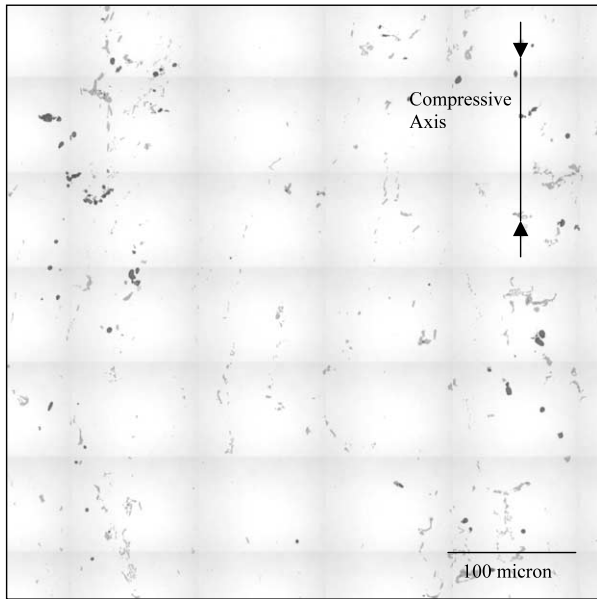


Fig. 3. Digitally compressed montage of $500 \times 500 \mu\text{m}^2$ area in 70% compression test 6061 Al-alloy specimen, originally grabbed at $50 \times$ objective magnification.

2. Experimental

2.1. Materials

The experiments were performed on the specimens drawn from extruded round bar (88 mm diameter) of 6061 Al-alloy in T651 condition. The material was supplied by ALCOA. The chemical composition of the alloy is given in Table 1.

2.2. Mechanical tests

Mechanical tests were performed on specimens extracted from the bar stock at a radial distance of 20 mm from the bar center through EDM. This was done in to ensure that the radial variations in microstructure and properties of the round bar did not influence testing results. All the specimens had their extrusion axis parallel to the applied load direction. Tension, compression, torsion, and notch-tension test specimens were machined from these cylindrical cores.

Interrupted uniaxial tensile tests were performed at different strain levels (including failure) on an MTS 880 servo-hydraulic test frame. The tensile test specimens were in the form of cylinders of 6.25 mm diameter and 25 mm length. These specimens were pulled in tension in a displacement-controlled rate of $5 \times 10^{-3} \text{ mm s}^{-1}$. Interrupted uniaxial compression tests were conducted at different strain levels up to 70% strain on an MTS81-Axial-Torsional servo-hydraulic test frame. These specimens were in the form of cylinders of 9 mm diameter and 12.5 mm length. Concentric grooves were machined into the ends of the compression cylinders in which a Mo based lubricant was placed. Lubrication was necessary in order to promote homogeneous deformation of the samples by lowering frictional effects at the sample ends. The samples were examined at the end of each test; no barreling effects were seen. Thus, homogeneous conditions are assumed for the compression tests. These quasi-static tests were run at strain rates of $2 \times 10^{-4} \text{ s}^{-1}$. Thick wall torsion samples were machined directly from the bar stock such that the wall of the samples coincided with the radial distance of 20

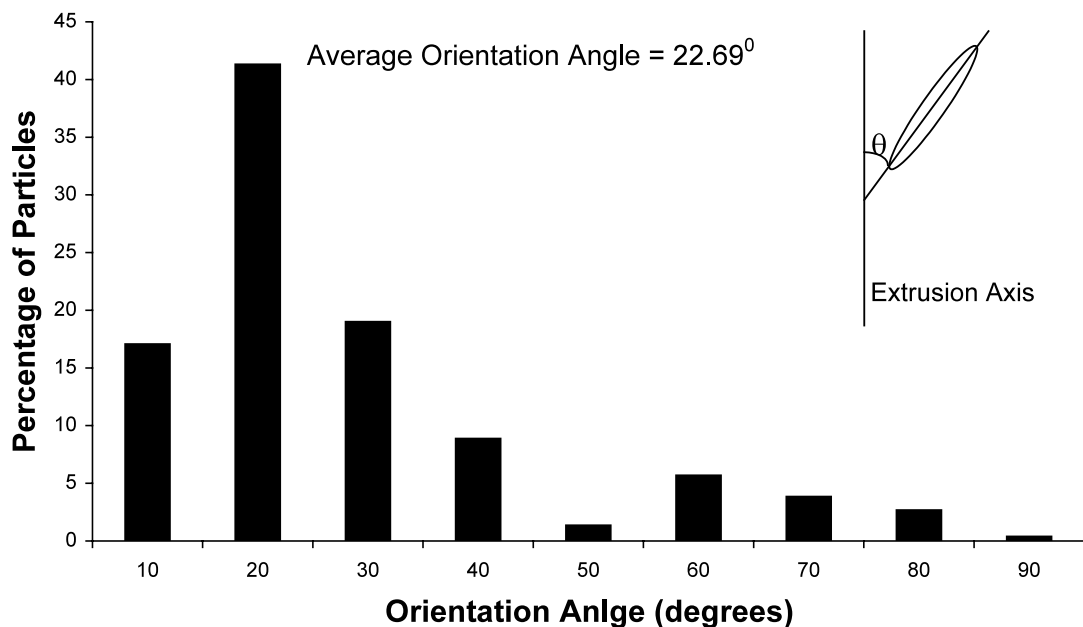


Fig. 4. Morphological orientation distribution of Fe-rich intermetallic particles in undeformed 6061 alloy.

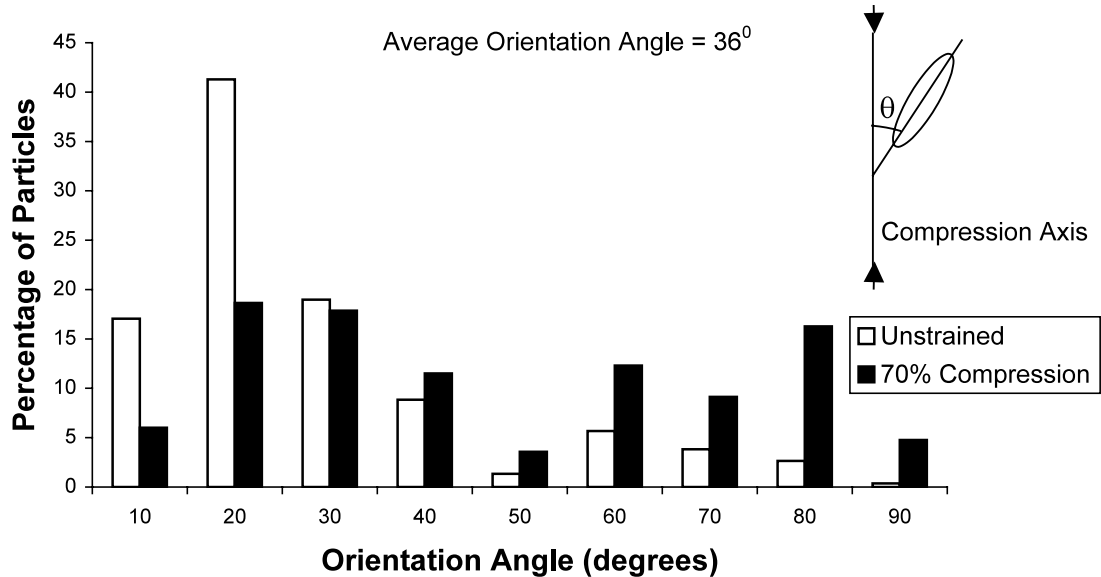


Fig. 5. Morphological orientation distribution of Fe-rich intermetallic particles in compression test specimen strained to 70% compressive strain.

mm from the bar center. Thus, the gage section of all samples corresponded to the same radial region of the bar stock material.

The effects of stress triaxiality were investigated through the use of notch-tensile tests. The gage section of these specimens was of 12.7 mm diameter containing a notch of 2.5 mm radius. The specimens were tested on an MTS 880 servo-hydraulic machine in a displacement-controlled mode. The specimens were tested to various percentages of the failure displacement.

2.3. Metallography

The specimens were cut in the center along vertical planes containing the applied load direction (torsion axis in the case of torsion test specimen) which was also the extrusion axis of the extruded bar. The samples were mounted and then polished by standard metallography techniques. The final polishing was done with 0.06- μm colloidal silica suspension to get the required metallographic finish. The specimens were observed under optical microscope in unetched condition.

2.4. Image analysis and quantitative metallography

Fig. 1 shows digital image microstructural montage of an unstrained specimen. The montage is a compressed digital image of $500 \times 500 \mu\text{m}^2$ area of a metallographic plane, created by cutting and pasting together numerous contiguous fields of view by using image-processing techniques. The microstructure contains two types of brittle particles in the aluminum matrix. Light gray particles are Fe-based intermetallics, and black equiaxed particles are Mg_2Si intermetallics. The Fe-rich gray particles are mostly oriented parallel to the extru-

sion axis, which is also the loading direction for all specimens. In the present study, the particle rotations of gray Fe-rich intermetallic particles are quantitatively characterized. In the present context, morphological orientation of a particle is defined as the angle between the major axis of a given particle and the loading direction (torsion axis in case of torsion test specimens), which is also the extrusion axis. In each specimen, these orientation angles were measured for about 5000 particles by using automatic image analysis. These measurements were performed on 350–400 contiguous microstructural fields (taken at $500\times$), to avoid any edge effects in the microstructural data. Morphological orientation distributions were computed from the image analysis data.

3. Results and discussion

Fig. 2 shows digital image microstructural montage of the torsion test specimen strained to 98% torsional

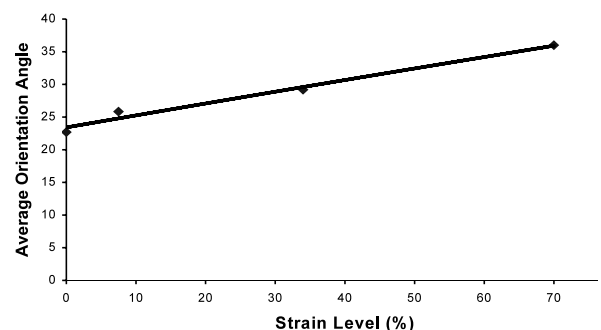


Fig. 6. Average orientation angle of Fe-rich intermetallic particles in 6061 Al-alloy under compression.

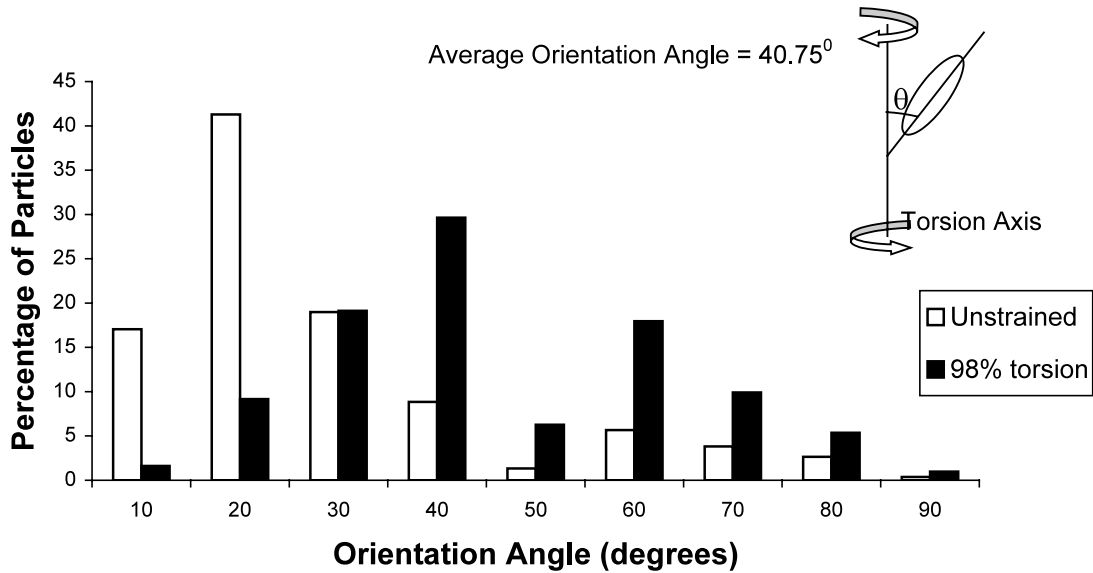


Fig. 7. Morphological orientation distribution of Fe-rich intermetallic particles in torsion test specimen strained to 98% torsion strain.

strain. The montage is a digitally compressed image of $500 \times 500 \mu\text{m}^2$ area of a vertical metallographic plane. In this image montage, torsion axis (which is the extrusion direction) is the Y-axis. Observe that, in the unstrained specimen (Fig. 1), the gray particles are mostly parallel to the extrusion direction (Y-axis), whereas, in the torsion tested specimen (Fig. 2) majority of the particles are oriented at an angle of about 45° with respect to the extrusion direction. Fig. 3 shows a digital image microstructural montage of the specimen strained to 70% strain in uniaxial compression. The montage is a digitally compressed image of $500 \times 500 \mu\text{m}^2$ area. Again, the Y-axis of the montage is the loading direction (and extrusion axis). In this specimen, some gray particles are oriented almost perpendicular to the loading direction. Such orientations are rare in the unstrained specimen (Fig. 1).

The morphological orientation distribution of the unstrained specimen (Fig. 4) reveals that about 77% of the particle orientations are in the range of $0\text{--}30^\circ$, and only 7% of the particles have orientation in the range of $60\text{--}90^\circ$. On the other hand, the morphological orientation distribution of the compression test (70% strain) specimen shown in Fig. 5 reveals that about 43% of the particles have their orientations in the range of $0\text{--}30^\circ$, and 30% of the particles are oriented at angles in the range of $60\text{--}90^\circ$ with respect to the loading direction. Further, the average orientation angle of the Fe-rich gray particles is 23° in the unstrained specimen, whereas, this average value is 36° for the compression test specimen (70% strain). Fig. 6 shows a plot of the average orientation angle of the particles versus strain for the compression test specimens. The average orientation angle monotonically increases with plastic strain under compression. These data clearly demonstrate that

the brittle Fe-rich gray particles rotate during the plastic deformation of the specimen under compressive load, and they tend to align themselves along the direction perpendicular to the loading axis, which is the direction of the induced tensile stress.

The orientation distribution of the particles in the torsion test specimen strained to 98% strain (Fig. 7) reveals that under torsional stress, 54% of the particles have their orientations in the range of $30\text{--}60^\circ$, whereas, in the unstrained specimen only 16% of particles have orientations in this range. The average orientation angle of the particles is 41° in this specimen as compared with 23° in the unstrained specimen. Fig. 8 shows the plot of average orientation angle of the particles versus torsional strain for the torsion test specimen. At least up to 98% torsion strain, the average appears to approach 45° with the increase in the strain. The data clearly show that significant particle rotations occur in torsion as well.

Inspection of the orientation distribution of the tensile test specimen (15.4% strain) shown in Fig. 9 reveals

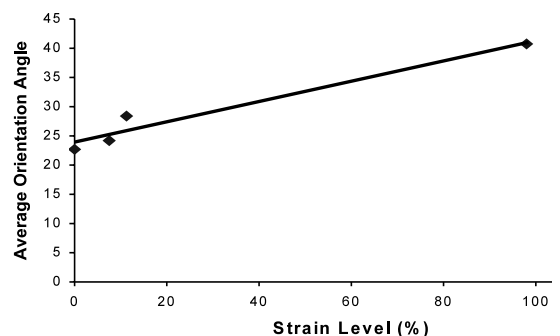


Fig. 8. Average orientation angle of Fe-rich intermetallic particles in 6061 Al-alloy under torsion.

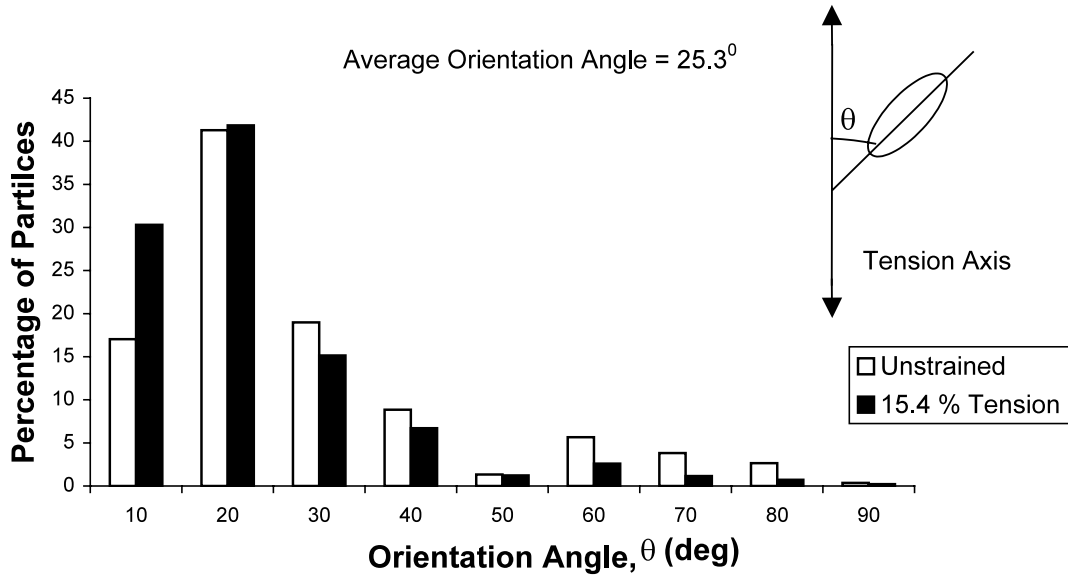


Fig. 9. Morphological orientation distribution of Fe-rich intermetallic particles in a uniaxial tension test specimen strained to 15.4% strain.

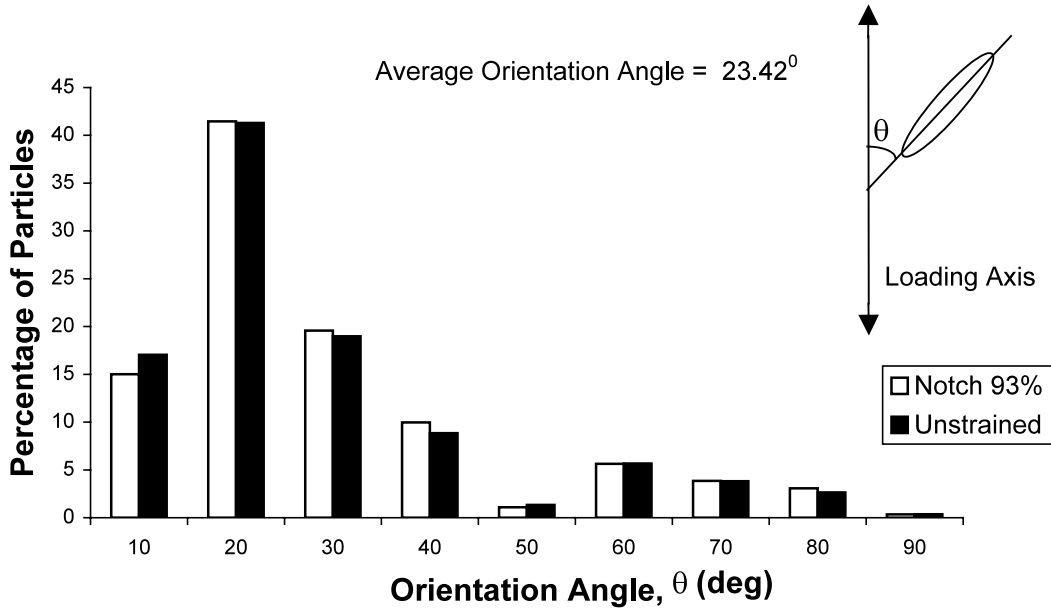


Fig. 10. Morphological orientation distribution of Fe-rich intermetallic particles in a notch-tension test specimen deformed to 93% of failure strain.

that there are 87% of the particles in the orientation range of $0-30^{\circ}$, as compared with 77% of the particles in this orientation range in the unstrained specimen. Therefore, under the tensile stress, particles rotate to align themselves parallel to the loading direction. However, in the unstrained specimen most of the particles are already aligned parallel to the extrusion axis (loading direction), and due to that, there is no drastic change in the orientation distribution of the tensile test specimen. Significant particle rotations would have occurred if the loading axis were perpendicular to the extrusion direction.

Fig. 10 shows the morphological orientation distribution of a notched tension test specimen having notch radius of 2.5 mm, and tested to 93% of failure displacement. Interestingly, there are no significant differences in the orientation distribution of the particles in this specimen as compared with those in the unstrained specimen. The average orientation angle of the particles in the notch tension specimen is 23° , which is equal to that in the unstrained specimen. In the notch-tension test specimen, the stress triaxiality is quite high (as compared with smooth tension test specimen), and therefore a significant tensile stress

component is present in all three principal directions, and a particle may rotate to align itself parallel to any one of the three such directions. Consequently, the morphological orientation distribution of the particles is not sensitive to these particle rotations.

The rotation of particles in deforming crystalline materials can be approached from several different points of view. If the particles are small with respect of the grain size, the particle rotations will be strongly influenced by the rotations of the grains. The local rotations of the grains and local compatibility of deformation governs the rotation of particles. Thus, issues such as grain size, local textures, particle size, spacing, aspect ratio, and initial orientations are expected to be important parameters in determining the rotations of particles. It is very likely that high aspect ratio particles with large inter-particle spacing may potentially undergo more rotations than equiaxed particles that are tightly spaced in the same ductile matrix. This is due to the fact that local deformations between the rigid particles can be accommodated much easier with sufficient spacing between the particles (more grains between particles). The rotation of particles and the factors that influence them become very important for modeling the differences in damage evolution under differing strain paths. The orientation of secondary phases with respect to the loading axis or principal stress directions may play a role in determining damage anisotropy. Consequently, modeling and tracking particle rotations must be included in ductile damage predictions that involve non-proportional loading or changes in strain path.

4. Conclusions

It is shown that significant rotations of anisotropic Fe-rich brittle particles occur during the plastic deformation of ductile Al-rich matrix in the 6061 Al-alloy. The particle rotations take place under all loading conditions. Under uniaxial tension and compression, the particles rotate to align themselves along the direction(s) of applied and induced tensile stress, respectively. In the case of torsion tests, at least up to 98% strain, the particles tend to align themselves at an angle of 45° with respect to the axis of torsion. The extent of particle rotations increases with the plastic strain, which may contribute significantly to the strain dependence of

the fraction of fractured particles, and consequently, to the strain dependence of the total microstructural damage. Therefore, the theories of damage nucleation via particle cracking should account for the particle rotations.

Acknowledgements

HA and AMG gratefully acknowledge the financial support from Sandia National Laboratories, Livermore, CA., and National Science Foundation (grant no. DMR-9816618) for this research.

References

- [1] A.M. Samuel, F.H. Samuel, *Metall. Mater. Trans.-A* 26A (1995) 2359.
- [2] E.N. Pan, C.S. Lin, C.R. Loper, *Am. Foundrymen Soc. Trans.* 98 (1990) 735.
- [3] Y. Jien-Wei, L. Wen-Pin, *Metall. Trans.-A* 27A (1996) 3558.
- [4] M.D. Dighe, M.S. Thesis Dissertation, Georgia Institute of Technology, 1999.
- [5] F.T. Lee, J.F. Major, F.H. Samuel, *Metall. Mater. Trans.-A* 26A (1995) 1553.
- [6] M.D. Dighe, A.M. Gokhale, M.F. Horstemeyer, *Metall. Mater. Trans.-A* 29A (1998) 905.
- [7] M.D. Dighe, A.M. Gokhale, M.F. Horstemeyer, *Metall. Mater. Trans.-A* 31 (2000) 1725.
- [8] J. Gurland, J. Plateau, *Trans. ASM* 56 (1963) 442.
- [9] C.H. Caceres, J.R. Griffiths, *Acta Mater.* 44 (1996) 25.
- [10] R. Doglione, J.L. Douzich, C. Berdin, D. Francois, *Mater. Sci. Forum.* (1996) 130.
- [11] M.F. Horstemeyer, A.M. Gokhale, *Int. J. Solids Struct.* 36 (1999) 5029.
- [12] M.F. Horstemeyer, J. Lathrop, A.M. Gokhale, M. Dighe, *Theor. Appl. Fracture Mech.* 33 (2000) 31.
- [13] C.H. Caceres, J.R. Griffiths, *Acta Mater.* 44 (1996) 25.
- [14] M.F. Ashby, *Phil. Mag.* 14 (1966) 1157.
- [15] J.P. Hirth, W.D. Nix, *Acta Metall.* 33 (1985) 359.
- [16] A.S. Argon, J. Im, R. Safoglu, *Metall. Trans.* 6A (1975) 825.
- [17] C.H. Caceres, C.J. Davidson, J.R. Griffiths, *Mater. Sci. Eng.* A197 (1995) 268.
- [18] B.A. Bilby, R. Bullough, E. Smith, *Proc. R. Soc. London A231* (1955) 263.
- [19] S. Prager, *Trans. Soc. Rheol.* 1 (1957) 53.
- [20] J.L. Erickson, *Arch. Rat. Mech. Anal.* 4 (1959) 231.
- [21] G.L. Hand, *J. Fluid Mech.* 33 (1962) 33.
- [22] S.G. Advani, C.L. Tucker, *J. Rheol.* 31 (1987) 751.
- [23] V.C. Prantil, J.T. Jenkins, P.R. Dawson, *J. Mech. Phys. Solids* 41 (1993) 1357.
- [24] G. Gonzalez-Doncel, O.D. Sherby, *Metall. Mater. Trans.* 27A (1996) 2837.
- [25] C. Schuh, D.C. Dunand, *Int. J. Plast.* 17 (2001) 317.